

MENSA: A Multi-Event Network for Survival Analysis under Informative Censoring

Christian Marius Lillelund*, Ali Hossein Gharari Foomani,
Weijie Sun, Shi-ang Qi, Russell Greiner

Department of Computing Science, University of Alberta, Edmonton, Canada
clillelund, hosseing, weijie2, shiang, rgreiner@ualberta.ca

Abstract

Given an instance, a multi-event survival model predicts the time until that instance experiences each of several different events. These events are not mutually exclusive and there are often statistical dependencies between them. There are relatively few multi-event survival results, most focusing on producing a simple risk score, rather than the time-to-event itself. To overcome these issues, we introduce *MENSA*, a novel, deep learning approach for multi-event survival analysis that can jointly learn representations of the input covariates and the dependence structure between events. As a practical motivation for multi-event survival analysis, we consider the problem of predicting the time until a patient with amyotrophic lateral sclerosis (ALS) loses various physical functions, *i.e.*, the ability to speak, swallow, write, or walk. When estimating when a patient is no longer able to swallow, our approach achieves an L1-Margin loss of 278.8 days, compared to 355.2 days when modeling each event separately. In addition, we also evaluate our approach in single-event and competing risk scenarios by modeling the censoring and event distributions as equal contributing factors in the optimization process, and show that our approach performs well across multiple benchmark datasets. The source code is available at: <https://github.com/thecml/mensa>

1 Introduction

Survival analysis models the probability that some event occurs at time T later than t (Gareth et al. 2021, Ch. 11). Here, we consider ways to learn such models, which is challenging, as the training dataset differs from standard regression datasets as it can include many censored instances – where we only have a lower bound on the actual time of the event. This problem can be extended to deal with many different events, such as the different loss of physical function that an ALS patient might suffer, or a competing risks setting, where the occurrence of one event excludes the others, such as predicting if a patient is going to die from breast cancer or heart failure. Traditionally, the Kaplan-Meier estimator (Kaplan and Meier 1958) or the Cox Proportional Hazards model (Cox 1972) have been used for multi-event problems – *e.g.*, Armstrong et al. (2014); Solomon et al. (2017), but modeling each event separately. These approaches do not

account for the relationships between events. There are also very few effective multi-event survival models in the literature, and most only deal with risk scores – *i.e.*, simply attempting to identify the order in which the subjects will die, thus there is a need for models that not only provide good discriminative performance (Tjandra, He, and Wiens 2021), but also accurate time-to-event estimates (Qi et al. 2023).

In this paper, we introduce *MENSA*, a novel **Multi-Event Network for Survival Analysis**, that jointly learns K event distributions as a convex combination of Weibull distributions. As a practical motivation for multi-event analysis, we consider the problem of predicting functional decline in patients suffering from amyotrophic lateral sclerosis (ALS) – which is a rapidly progressing motor neuron disease with a medium survival time of 3 to 5 years. However, instead of simply predicting the time to death (Kjældgaard et al. 2021; Kuan et al. 2023), we predict when events related to a lack of physical function will occur. This information can be used to design personalized treatment plans and provide insight into disease mechanisms. We also evaluate our model in single-event and competing risks scenarios, and address these issues with a new approach inspired by the multi-event problem: Instead of considering censoring to be non-informative, *i.e.*, the distribution of event times provides no information about the distribution of censoring times, we model censoring explicitly as if it were another event and perform likelihood estimation in conjunction. This allows practitioners to predict censoring – *e.g.*, predict when a patient is going to drop out or prematurely leave a study. We show that our approach improves over state-of-the-art baselines in single and competing risks in multiple datasets in terms of L1-Margin loss. In summary, our contributions are the following:

- We propose *MENSA*, a novel, deep learning approach for multi-event survival analysis, that models events jointly as a convex combination of Weibull distributions.
- We adopt our method to single-event and competing risks by treating the event and censoring distributions as equal factors during model training. This enables predicting if an instance will likely experience the event of interest or be censored, *e.g.*, drop out of the study or be event-free at its termination.
- We evaluate the approaches in four real-world datasets and show that our method performs well across multiple benchmark datasets, especially for L1-Margin loss.

*Corresponding author.

2 Background and Related Work

Below we provide a brief overview of relevant literature in competing risks, multi-event survival analysis, and dependent censoring using copulas.

Competing Risks Survival Analysis

Competing risks is a form of dependent censoring, where the occurrence of one event can be prevented by another (Emura and Chen 2018, Ch. 1). Thus, competing risks data do not allow us to observe the times for both events for any subject, and hence, it is not possible to identify the dependence structure from the data alone (Tsiatis 1975). Multiple works have addressed dependencies among related survival outcomes, usually assuming that competing risks are conditional independent given the covariates – *i.e.*, $T_k \perp T_{i:i \neq k} \mid X$, where the random variable T_k is the time of the k^{th} event, and X are the observed covariates.

Lee et al. (2018) proposed DeepHit, a multilayer perceptron (MLP) for competing risks, which learns the joint distribution of events. The idea of learning competing events jointly has since been extended to longitudinal data (Lee and et al. 2019), or using the multi-task logistic regression (MTLR-CR) framework for competing risks (Kim, Kazmierski, and Haibe-Kains 2021).

Nagpal, Li, and Dubrawski (2021) proposed Deep Survival Machines (DSM), a parametric survival model that first learns a common representation of all competing risks, and then a k th-event distribution for a single event using cause-specific maximum likelihood estimation (MLE), treating all other events than k as censored. This approach does not account for the density or survival function of the censoring distribution, and consequently, any potential interdependencies between the event and the censoring distribution are not addressed.

Multi-Event Survival Analysis

Given an instance, a multi-event survival model predicts the time until that instance experiences each of several events, which are not mutually exclusive, but are assumed to have some prior relationship. For example, once a patient is diagnosed with lung cancer, we anticipate that patient will soon be diagnosed with pneumonia.

Larson (1984) adopted the popular Cox Proportional Hazards model (CoxPH) (Cox 1972) for multi-event survival analysis by modeling each event separately; this approach has been used in several works since (Armstrong et al. 2014; Solomon et al. 2017), but generally fails to capture the dependencies between events.

Andersen and Keiding (2002) proposed a multi-state model that learns a model for each event transition (*e.g.*, given a person is diagnosed with lung cancer, then predict the probability of pneumonia), but this approach can only learn the bijective relationship between two events, meaning it cannot leverage shared information among more than two events. Several works have addressed this restriction – *e.g.*, using a shared frailty term across models (Jiang and Haneuse 2017), applying forms of regularization (Li et al. 2016; Wang et al. 2017) or by modeling the joint survival

distribution (Hsieh and Wang 2018). However, these methods require specific assumptions regarding the distribution of the frailty term, the proportional hazards assumption, or the structure of the joint survival distribution, respectively.

Tjandra, He, and Wiens (2021) proposed a hierarchical multi-event model that learns the probability of event occurrence at different hierarchical time scales, using coarse predictions to iteratively guide predictions at finer and finer level – *e.g.*, from monthly to daily predictions. The method shows promising discriminative in synthetic data for discrimination proposes (*i.e.*, ranking), but lacks evaluation in a real-world dataset.

Dependent Censoring and Copulas

Dependent censoring is a type of informative censoring where the dependence between the censoring time and the survival time is not explained by any observable covariate (Emura and Chen 2018, Ch. 1). In other words, dependent censoring is a consequence of some residual dependence – *i.e.*, when covariates influencing both survival time and censoring time are ignored or not included in the analysis. A copula is a function that links two random variables by specifying their dependence structure (Emura and Chen 2018, Ch. 1), thus it can be applied to introduce a dependence between the event and the censoring distribution. The propose of the copula in this work is to investigate our proposed method under dependent censoring.

Formally, we write $C(u_1, \dots, u_d) : [0, 1]^d \rightarrow [0, 1]$, which is a d -dimensional copula (*i.e.*, where d is the number of variables) with u_1, \dots, u_d uniform marginal probabilities. For simplicity, we initially assume the single event case, where T_E is the event time, T_C is the censoring time, \mathbf{x} is a vector of covariates, and $S_{T_E}(t \mid \mathbf{x}) = \Pr(T_E > t_e \mid \mathbf{x})$ and $S_{T_C}(u \mid \mathbf{x}) = \Pr(T_C > t_c \mid \mathbf{x})$ are the marginal survival functions given \mathbf{x} . We can then define a bivariate survival copula (Emura and Chen 2018, Ch. 3) C_θ that describes the degree of dependence between T_E and T_C :

$$\Pr(T_E > t_e, T_C > t_c \mid \mathbf{x}) = C_\theta\{S_{T_E}(t_e \mid \mathbf{x}), S_{T_C}(t_c \mid \mathbf{x})\}. \quad (1)$$

If C_θ satisfies certain mathematical conditions, then Eq. (1) is a valid survival function (Emura and Chen 2018, Ch. 3). Kendall’s tau (τ) is a common measure of the dependency between T_E and T_C , which is defined by:

$$\tau = \Pr\{(T_2 - T_1)(C_2 - C_1) \geq 0 \mid \mathbf{x}\} - \Pr\{(T_2 - T_1)(C_2 - C_1) < 0 \mid \mathbf{x}\}, \quad (2)$$

where (T_1, C_1) and (T_2, C_2) are sampled from the model (1). In this work, we will use Archimedean copulas – *e.g.*, Clayton or Frank – each parameterized by a single parameter, θ , to introduce dependence between the event and censoring distributions. An Archimedean copula is defined by:

$$C_\theta(u, v) = \varphi_\theta^{-1}(\varphi_\theta(u) + \varphi_\theta(v)), \quad (3)$$

where the function $\varphi_\theta : [0, 1] \rightarrow [0, 1]$ is called a generator of the copula, which is continuous and strictly decreasing from $\varphi_\theta(0) \geq 0$ to $\varphi_\theta(1) = 0$ (Emura and Chen 2018, Ch. 3).

3 Methods

Survival Analysis and Notation

Survival analysis models the time until some events of interest occur, which can be partially observed due to censoring, e.g., termination of the study or dropout (Gareth et al. 2021, Ch. 11). Let $\mathcal{D} = \{(\mathbf{x}^{(i)}, \mathbf{t}^{(i)}, \delta^{(i)})\}_{i=1}^N$ be the dataset, where $\mathbf{t}^{(i)} \in \{1, 2, \dots, T_{\max}\}^K$ is a vector of observed times for the i -th person across K different events, each at some time, $\delta^{(i)} \in \{0, 1\}^K$ is vector of event indicators for each event, and $\mathbf{x}^{(i)} \in \mathbb{R}^d$ is a d -dimensional vector of features (covariates). Moreover, let $e_k^{(i)} \in \{1, 2, \dots, T_{\max}\}^K$ denote event times and $c_k^{(i)} \in \{1, 2, \dots, T_{\max}\}^K$ denote censoring times for event k over the event horizon, thus $t_k^{(i)} = e_k^{(i)}$ if $\delta_k^{(i)} = 1$, otherwise, $t_k^{(i)} = c_k^{(i)}$ if $\delta_k^{(i)} = 0$.

In a competing risks scenario, only one event or the censoring can be observed. We define a survival problem as predicting the probability of event k at each time point $t \in \{1, 2, \dots, T_{\max}\}$, thus producing a matrix of so-called survival functions $\mathbf{S}^{(i)} = \{s_1^{(i)}, s_2^{(i)}, \dots, s_K^{(i)}\}$ for patient i . The survival function $S(t | X)$ is the probability that some event occurs at time T later than t - i.e., $s_k^{(i)} = (P(e_k^{(i)} > 1), P(e_k^{(i)} > 2), \dots, P(e_k^{(i)} > T_{\max}))$ describes the probability of individual i not having event k until t for $t \in \{1, 2, \dots, T_{\max}\}$, and is not increasing for $t > 0$. Omitting k for brevity, let $f_{T|X}(\cdot)$ and $F_{T|X}(\cdot)$ represent the conditional density and cumulative distribution functions, respectively, over the event horizon, with the event distribution T_E and the censoring distribution T_C . Then we have the following definitions:

Definition 1 The survival function

$$S_{T|X}(t | X) = \Pr(T > t | X) = 1 - F_{T|X}(t | X), \quad (4)$$

represents the probability the event occurs at time t (Gareth et al. 2021, Ch. 11).

Definition 2 The hazard function

$$\begin{aligned} h_{T|X}(t | X) &= \lim_{\epsilon \rightarrow 0} \Pr(T \in [t, t + \epsilon) | T \geq t, X) \\ &= \frac{f_{T|X}(t | X)}{S_{T|X}(t | X)}, \end{aligned} \quad (5)$$

represents the instantaneous event rate at given time t , conditional on surviving t (Gareth et al. 2021, Ch. 11).

Definition 3 The likelihood function

$$\begin{aligned} \mathcal{L}(\mathcal{D}) &= \Pr(T_E = t, T_C \geq t | \mathbf{x}^{(i)})^{\delta^{(i)}} \times \\ &\quad \Pr(T_E \geq t_i, T_C = t_i | \mathbf{x}^{(i)})^{1-\delta^{(i)}}, \end{aligned} \quad (6)$$

represents the likelihood for the i -th patient given the data $\mathcal{D} = \{(X^{(i)}, T^{(i)}, \delta^{(i)})\}_{i=1}^N$ under informative censoring (Gareth et al. 2021, Ch. 11).

The Proposed Method

Our method is an extension of DSM (Nagpal, Li, and Dubrawski 2021), which can handle competing risks, but does not incorporate the censoring distribution as part of the loss function and does not address any potential relationship between the two, i.e., it assumes non-informative censoring.

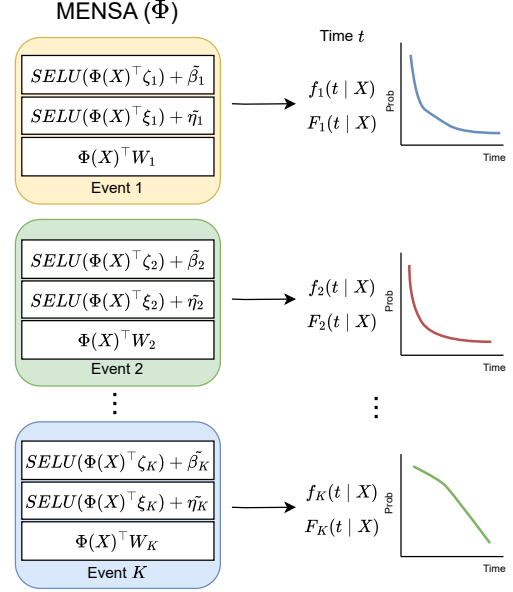


Figure 1: The proposed architecture for multi-event survival prediction. The model generates survival distributions for K different events based on patient covariates, X . Φ represents the shared MLP layer that processes these covariates and supports the prediction of survival outcomes across all K events.

MENSAs. We propose to model the marginal survival distribution for each event and the censoring distribution as a convex combination of Weibull distributions. There are two primary reasons for this: (1) this approach relaxes any assumption about the underlying marginal survival distribution for each event, and (2) a continuous survival model enables the use of a copula during training in the future. We also emphasize that the Weibull distribution has a closed-form cumulative distribution function (CDF) and probability density function (PDF), which eases the gradient computation. For each Weibull distribution in our model, the PDF and CDF can be calculated as:

$$f(t; \beta, \eta) = \frac{\eta}{\beta} \left(\frac{t}{\beta}\right)^{\eta-1} e^{-\left(\frac{t}{\beta}\right)^\eta}, \quad (7)$$

$$F(t; \beta, \eta) = 1 - e^{-\left(\frac{t}{\beta}\right)^\eta}. \quad (8)$$

Assuming our estimated survival distribution is a convex combination of M different Weibulls for each marginal distribution, we define the log of β_m and η_m as:

$$\log(\beta_m(\mathbf{x}^{(i)})) = \tilde{\beta}_m + \text{SELU}(\Phi_\theta(\mathbf{x}^{(i)})^\top \zeta_m), \quad (9)$$

$$\log(\eta_m(\mathbf{x}^{(i)})) = \tilde{\eta}_m + \text{SELU}(\Phi_\theta(\mathbf{x}^{(i)})^\top \xi_m). \quad (10)$$

where SELU is the Scaled Exponential Linear Units activation function. As a result, we define the CDF and PDF for

each marginal distribution as:

$$F(t_i; \beta, \eta, \mathbf{x}^{(i)}) = \sum_{m=1}^M W_m(\mathbf{x}^{(i)}) F_m(t_i; \beta_m(\mathbf{x}^{(i)}), \eta_m(\mathbf{x}^{(i)})),$$

$$f(t; \beta, \eta, \mathbf{x}^{(i)}) = \sum_{m=1}^M W_m(\mathbf{x}^{(i)}) f_m(t; \beta_m(\mathbf{x}^{(i)}), \eta_m(\mathbf{x}^{(i)})),$$

$$\text{where } W = \text{Softmax}(\Phi_\theta(\mathbf{x}^{(i)})^\top \theta_w).$$

Here, $\mathbf{x}^{(i)}$ is a vector of covariates for each instance and $\Phi(\cdot)$ is a multilayer perceptron (MLP). $\{\theta, \tilde{\beta}, \tilde{\eta}, \zeta, \xi, \theta_w\}$ are the parameters of the model that can be learned jointly during optimization using maximum likelihood estimation (MLE). Algorithm 1 shows the optimization procedure.

MLE for Competing Risks. Under the conditional independence assumption, we can write the survival likelihood for the dataset $\mathcal{D} = \{(\mathbf{x}^{(i)}, \mathbf{t}^{(i)}, \delta^{(i)})\}_{i=1}^N$ as:

$$\mathcal{L}(D) = \prod_{i=1}^N \prod_{j=1}^K f_{T_{E_j}|X}(T_{\text{obs}}^{(i)} | X^{(i)})^{\delta_j^{(i)}} S_{T_{E_j}|X}(T_{\text{obs}}^{(i)} | X^{(i)})^{1-\delta_j^{(i)}}, \quad (11)$$

where N is the number of samples, K is the number of events including censoring, and $\delta_j^{(i)}$ indicates the event indicator for j th event for the i th sample. We then optimize the joint log-likelihood function, which has the following form:

$$\mathcal{L}(D) = \sum_{i=1}^N \sum_{j=1}^K \delta_j^{(i)} f_{T_{E_j}|X}(T_{\text{obs}}^{(i)} | X^{(i)}) + (1 - \delta_j^{(i)}) S_{T_{E_j}|X}(T_{\text{obs}}^{(i)} | X^{(i)}). \quad (12)$$

In (Eq. 12), we model each competing risk separately as a convex combination of Weibull distributions and combine it in a composite loss function. The main differences between our approach and DSM is that we include the censoring distribution as an event in the loss function, and optimize the log-likelihood directly instead of deriving a lower bound on it.

MLE for Multi-event. Now we describe the modifications required to extend our model to the multi-event scenario. In multi-event survival analysis, the K events of interest can happen in any order and at any time, thus they are not mutually-exclusive as in competing risks. As a result, each k -event can be observed at different times. Considering these differences, we define the objective function in a multi-event scenario as composite:

$$\mathcal{L}(D) = \sum_{i=1}^N \sum_{j=1}^K \left[\delta_j^{(i)} f_{T_{E_j}|X}(T_{\text{obs}(j)}^{(i)} | X^{(i)}) + (1 - \delta_j^{(i)}) S_{T_{E_j}|X}(T_{\text{obs}(j)}^{(i)} | X^{(i)}) \right],$$

where $T_{\text{obs}(j)}^{(i)}$ indicates the observed time for j th event.

Algorithm 1 Optimizing the likelihood in MENSA using Adam (Kingma and Ba 2017) over N samples and K events.

- 1: **Input:** a survival dataset \mathcal{D} of the form $\{(X^{(i)}, T_{\text{obs}}^{(i)}, \delta^{(i)})\}_{i=1}^N$; \mathcal{M} : the proposed MENSA model parameterized by $\{\theta, \tilde{\beta}, \tilde{\eta}, \zeta, \xi, \theta_w\}$; α : learning rate for the model; B : number of training epochs.
 - 2: **Result:** $\{\hat{\theta}, \hat{\beta}, \hat{\eta}, \hat{\zeta}, \hat{\xi}, \hat{\theta}_w\}$: The learned parameters of the model.
 - 3: **Initialization:**
 $\mathcal{M} \leftarrow \text{Instantiate}(\mathcal{M}; \hat{\theta}^{(0)}, \hat{\beta}^{(0)}, \hat{\eta}^{(0)}, \hat{\zeta}^{(0)}, \hat{\xi}^{(0)}, \hat{\theta}_w^{(0)})$
 - 4: **for** $i = 1, \dots, B$ **do**
 - 5: $f(T_{\text{obs}}), S(T_{\text{obs}}) \leftarrow \mathcal{M}(\mathcal{D})$ // f, S are $N * K$, where K is the number of events
 - 6: $\mathcal{L}_i \leftarrow \ell(\delta_{n=1}^N, f(T_{\text{obs}}), S_{T_{\text{obs}}})$
 - 7: $\hat{\theta}^{(i)} \leftarrow \text{Adam}(\hat{\theta}^{(i-1)}, \mathcal{L}_i, \alpha)$
 - 8: $\hat{\beta}^{(i)} \leftarrow \text{Adam}(\hat{\beta}^{(i-1)}, \mathcal{L}_i, \alpha)$
 - 9: $\hat{\eta}^{(i)} \leftarrow \text{Adam}(\hat{\eta}^{(i-1)}, \mathcal{L}_i, \alpha)$
 - 10: $\hat{\zeta}^{(i)} \leftarrow \text{Adam}(\hat{\zeta}^{(i-1)}, \mathcal{L}_i, \alpha)$
 - 11: $\hat{\xi}^{(i)} \leftarrow \text{Adam}(\hat{\xi}^{(i-1)}, \mathcal{L}_i, \alpha)$
 - 12: $\hat{\theta}_w^{(i)} \leftarrow \text{Adam}(\hat{\theta}_w^{(i-1)}, \mathcal{L}_i, \alpha)$
 - 13: **end for**
 - 14: **Output:** $\{\hat{\theta}^{(i)}, \hat{\beta}^{(i)}, \hat{\eta}^{(i)}, \hat{\zeta}^{(i)}, \hat{\xi}^{(i)}, \hat{\theta}_w^{(i)}\}$
-

4 Experimental Setup

We evaluate our approach across different datasets and compare to literature benchmarks.

Datasets

Synthetic: Following the approach of Foomani et al. (2023), we create synthetic datasets from a data generation process with a linear or nonlinear activation function. The event and censoring distributions are specified by Weibull marginal distributions for a single-event setting. Specifically, we sample K random variables from a known copula given by Kendall's τ . If $\tau = 0$, the marginals are generated as independent uniform random variables. If $\tau > 0$, the marginals are generated using an Archimedean copula (e.g., Clayton or Frank) to introduce dependence. We then apply inverse transform sampling to generate event times $e_k^{(i)}$ according to their Weibull distribution parameters given by $\alpha_k = \{17, 18\}$ and $\gamma_k = \{5, 4\}$. The observed time is the minimum of the generated event times, i.e., $t_k^{(i)} = \min_k e_k^{(i)}$ and $\delta^{(i)} = k$ for the i -th instance. We generate $N = 5,000$ samples for each experiment with $d = 10$ covariates. More details are given in the Supplement.

MIMIC-IV: The Medical The Information Mart for Intensive Care (MIMIC-IV) dataset comprises electronic health records from patients admitted to intensive care units at the Beth Israel Deaconess Medical Center in the United States, covering the years 2008 to 2019 (Johnson et al. 2023). Using the method described in Gupta et al. (2022), we have extracted 1,672 static features from the MIMIC-IV dataset, which includes data from 26,236 patients whose age between 60 and 65 years. To refine our feature set, we

applied the uniox feature selection method (Qi et al. 2022; Simon et al. 2003), reducing the number of covariates to 100 that are highly relevant. The event of interest is death since hospital admission.

SEER: The U.S. Surveillance, Epidemiology, and End Results (SEER) dataset contains survival times for cancer patients (Gloeckler Ries et al. 2003). We select a cohort of 19,246 newly-diagnosed patients (first year of disease) with 17 covariates, which include demographics and tumor characteristic. For the single event case, we consider the outcome of death due to breast cancer, and for competing risks, we consider the outcomes of death due to breast cancer and death due to heart failure, other outcomes being censored.

Rotterdam: The Rotterdam dataset (Royston and Altman 2013) contains records of 2,982 primary breast cancer patients, whose records were included in the Rotterdam tumor bank, of whom 1546 had node-positive disease. The dataset has 10 covariates, which include demographics, tumor characteristics, and treatment information. We consider the survival time as the time from primary surgery to the earlier of disease recurrence or death from any cause, *i.e.*, two competing risks and censoring.

PRO-ACT: The Pooled Resources Open-Access Clinical Trials (PRO-ACT)¹ (Atassi et al. 2014) database is the largest ALS dataset in the world. It includes patient demographics, lab and medical records and family history of over 11,600 ALS patients. ALS disease state is evaluated by the ALS functional rating scale (ALSFRS), which consists of ten items, each representing physical functionality, *e.g.*, the ability to walk. Each ALSFRS score is between 0 and 4, where 0 represents complete inability with regard to the function, and 4 represents normal function. We use the ALSFRS scores to formulate four distinct events: “Speech”, “Swallowing”, “Handwriting” and “Walking”. We consider an event to have occurred if a patient scores 2 or lower on the ALSFRS scale during any subsequent follow-up visitation following their initial visitation. The events can occur in any order and are non-mutually exclusive. Since the mean survival time with ALS is two to five years, we use a maximum follow-up time of 1000 days (approx. 2.7 years) in our study. The dataset has 3,865 observations, 15 covariates and four separate, but related events.

Baselines

DeepSurv: DeepSurv (Katzman et al. 2018) is a Cox proportional hazards (CoxPH) (Cox 1972) MLP of the form $h(t|\mathbf{x}_i) = h_0(t) \exp(f(\boldsymbol{\theta}, \mathbf{x}_i))$, where $f(\boldsymbol{\theta}, \mathbf{x}_i)$ denotes a risk score as a nonlinear function of the covariates, *i.e.*, $f(\boldsymbol{\theta}, \mathbf{x}_i) = \sigma(\mathbf{x}_i \boldsymbol{\theta})$. The MLE for $\hat{\boldsymbol{\theta}}$ is derived by numerically maximizing the partial log-likelihood. Note that this estimator is biased under residual dependence (Emura and Chen 2018, Ch. 1). DeepSurv supports single-event only.

RSF: Random Survival Forests (RSF) (Ishwaran et al. 2008) extends decision trees for survival analysis. It works

¹Data used in the preparation of this article were obtained from the Pooled Resource Open-Access ALS Clinical Trials (PRO-ACT) Database. The data available in the PRO-ACT Database have been volunteered by PRO-ACT Consortium members.

Dataset	N	d	K	Event distribution %:
Synthetic	5,000	10	2	C: 61.5, E: 38.5
MIMIC-IV	26,236	100	2	C: 62.8, D: 37.2
SEER	19,246	17	2 3	C: 54.2, D: 45.5 C: 42.1, BC: 12.4, HF: 45.5
Rotterdam	2,982	10	3	C: 42.6, R: 6.5, D: 50.9
PRO-ACT	3,865	15	4	SP: 54.2, SW: 49.2 HA: 60.3, WA: 75.0

Table 1: Overview of the datasets. N is the number of samples and d is the number of covariates. In MIMIC-IV, ‘C’ denotes the censoring event and ‘D’ denotes the death event. In SEER, ‘C’, ‘BC’ and ‘HF’ denote the censoring event, death by breast cancer and death by heart failure, respectively. In Rotterdam, ‘R’ means relapse and ‘D’ means death. In PRO-ACT, ‘SP’, ‘SW’, ‘HA’ and ‘WA’ are the speech, swallowing, handwriting and walking events, respectively.

similarly to regular Random Forests by recursively partitioning data based on some splitting criterion. Each tree is built on a different bootstrap sample, evaluating only a random subset of features at each node. Predictions are then made by aggregating the outputs of all trees.

DeepHit: DeepHit (Lee et al. 2018) is a discrete-time survival model designed to handle competing risks. It features a shared sub-network among all events and cause-specific sub-networks for each competing event. The model outputs a probability distribution for each discrete time bin and each competing event via a softmax layer. This architecture allows DeepHit to learn the joint distribution of survival times and events directly, without making assumptions about the underlying stochastic process.

DSM: Deep Survival Machines (DSM) (Nagpal, Li, and Dubrawski 2021) models the survival distribution as a mixture of some fixed k parametric distributions. The parameters of these mixture distributions and the mixing weights are estimated using an MLP. DSM supports single-event and competing risks.

DCSurvival: DCSurvival (Zhang, Ling, and Zhang 2024) is a copula-based survival model that supports dependent censoring without having to specify the ground truth copula in advance, assuming it is Archimedean. It learns the copula C_θ through a generator function ϕ_θ as a finite sum of negative exponentials, which are the parameters of an MLP (Ling, Fang, and Kolter 2020). DCSurvival supports single-event only.

Hierarchical: The hierarchical survival model (Tjandra, He, and Wiens 2021) learns the survival distribution by iteratively predicting the probability of event at increasingly finer time scales. During training, the model uses a composite loss function using ranking penalties that provide supervision across the entire prediction horizon. Hierarchical supports competing risks and multi-event settings.

MTLR: The Multi-Task Logistic Regression (MTLR) model (Yu et al. 2011) predicts the survival distribution us-

ing a sequence of dependent logistic regressors. It discretizes the event horizon into bins, and estimates the probability of event at each bin. MTLR has been extended to competing risks as Deep-CR MTLR (Kim, Kazmierski, and Haibe-Kains 2021).

Evaluation

We adopt several evaluation metrics to assess the performance of our method and literature benchmarks. To evaluate discrimination performance, we report the traditional Harrell’s concordance-index (Harrell Jr, Lee, and Mark 1996), a global concordance-index as the average of the concordance indices across all events, and a local concordance-index as the average of the concordance indices for each individual per event. To evaluate prediction performance, we report the mean absolute error (MAE) using a L1-Margin loss for censored individuals (mMAE) (Haider et al. 2020) and the Integrated Brier Score (IBS) (Graf et al. 1999). To evaluate the calibration performance, we report the Distribution-Calibration (D-Cal) score (Haider et al. 2020), which measures how well the survival function is calibrated for each event, *i.e.*, do the time-of-event empirical quantiles match the predicted probabilities. Lastly, we evaluate the bias induced by dependent censoring using the Survival- ℓ_1 error (Foomani et al. 2023), which is the ℓ_1 distance between the ground truth survival curve and the estimated survival curve. More details on the evaluation metrics are given in the Supplement.

Implementation

As described, we propose a multilayer perceptron (MLP) as the backbone network architecture for our mixture model. An MLP is a fully connected feedforward network with a number of hidden layers and a nonlinear activation function. The use of an MLP is consistent with the literature, showing strong predictive performance (Katzman et al. 2018; Nagpal, Li, and Dubrawski 2021; Lillielund, Magris, and Pedersen 2024). We use a single layer with $\{32, 64, 128\}$ nodes and the ReLU6 activation function. For all experiments, we train MENSA with the Adam optimizer (Kingma and Ba 2017) using learning rates of $\{1e-3, 5e-4, 1e-4\}$ for the MLP, and $\{1, 3, 5\}$ number of Weibull distributions. Training is done using minibatches, *i.e.*, stochastic subsets of the training dataset with sizes of $\{32, 64, 128\}$. All experiments were conducted in PyTorch (Paszke et al. 2019) using double precision (fp64) for tensor computation. How to replicate the results are detailed in the Supplement.

After imputing missing values by sample mean for real-valued covariates or mode for categorical covariates, we apply a z -score data normalization for real-world datasets and use one-hot encoding for categorical covariates. We split the data into train, validation and test sets by 70%, 10%, and 20% using a stratified procedure using a random seed. We run every experiment five times with different seeds, and every algorithm use the same training, validation and test sample. The stratification ensures that the event times are consistent across the three sets. During training, we use early stopping based on the performance of the validation set.

5 Results and Takeaways

Here, we evaluate the proposed approach for single-event, competing risks and multi-event applications.

Single-event prediction

To investigate our approach under dependent censoring, we artificially create a synthetic regression dataset according to various degrees of dependence from a copula, *e.g.*, Frank, Clayton. We generate two datasets, Linear-Risk and Nonlinear-Risk, which correspond to cases where the Weibull hazards are linear and non-linear functions of covariates. Figure 2 plots the bias incurred by our approach and baseline methods under dependent censoring. All baseline models are configured with sensible defaults. We see that MENSA has one of the lowest Survival- ℓ_1 in the linear cases, and is on par with the state-of-the-art models in the nonlinear cases. Moreover, introducing dependent censoring does not seem to have a detrimental in terms of the Survival- ℓ_1 error in the nonlinear cases, and the algorithms are generally aligned in this situation.

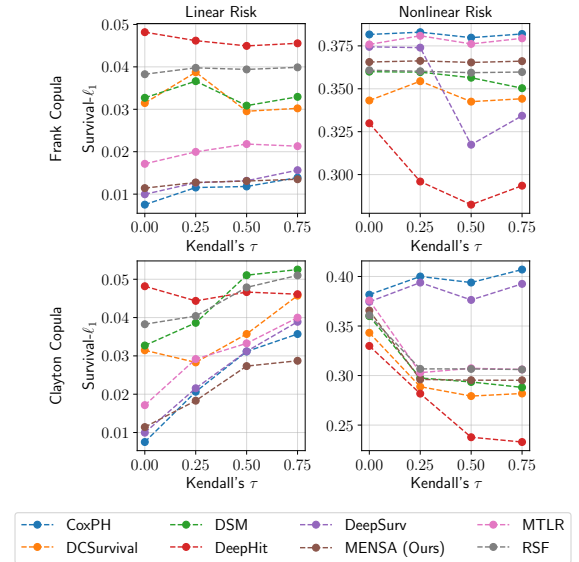


Figure 2: Plot of survival prediction biases as a function of Kendall’s τ . The lines represent the Survival- ℓ_1 means over 5 experiments.

Table 3 shows model performance in the single event case in the SEER and MIMIC-IV test sets. Here, MENSA improves over all rival methods in the SEER dataset, and has the best Harrell’s concordance-index and mMAE in the MIMIC-IV dataset. We were not able to compare DCSurvival in these two datasets since the model did not converge.

Competing risks prediction

Table 2 shows the performance of our proposed method, and literature benchmarks on the test sets under competing risks. In the large SEER dataset, our method shows similar discriminative performance in terms of the concordance-index as the baseline DeepSurv MLP, however, it has the lowest mMAE across the two events of interest, death by breast

Dataset	Method	Harrell’s CI	IBS	mMAE	Global CI	Local CI	D-Cal
(SEER $N = 19,246$, $d = 17$, $K = 3$)	DeepSurv (indep.)	0.69±0.01	0.12±0.00	30.52±0.94	0.74±0.00	0.79±0.01	(5/5, 0/5)
	DeepHit	0.66±0.01	0.14±0.00	75.44±5.21	0.72±0.00	0.78±0.00	(0/5, 0/5)
	Hierarch.	0.66±0.02	0.16±0.00	36.17±1.01	0.71±0.01	0.71±0.01	(0/5, 0/5)
	MTLR-CR	0.62±0.01	0.16±0.00	37.76±0.62	0.66±0.01	0.75±0.01	(0/5, 0/5)
	DSM	0.67±0.02	0.13±0.00	68.32±8.93	0.72±0.01	0.80±0.00	(5/5, 1/5)
	MENSA (Ours)	0.67±0.01	0.12±0.00	25.76±0.42	0.73±0.00	0.79±0.01	(5/5, 5/5)
(Rotterdam $N = 2,982$, $d = 10$, $K = 3$)	DeepSurv (indep.)	0.75±0.02	0.14±0.04	488.0±215.0	0.68±0.01	0.87±0.02	(5/5, 5/5)
	DeepHit	0.69±0.03	0.16±0.04	31.06±7.05	0.63±0.03	0.89±0.02	(4/5, 2/5)
	Hierarch.	0.74±0.02	0.78±0.18	83.56±9.03	0.68±0.01	0.85±0.03	(0/5, 0/5)
	MTLR-CR	0.75±0.01	0.16±0.06	52.39±8.48	0.68±0.01	0.86±0.02	(1/5, 2/5)
	DSM	0.73±0.03	0.15±0.03	266.01±5.34	0.68±0.01	0.86±0.04	(5/5, 3/5)
	MENSA (Ours)	0.73±0.01	0.16±0.07	53.40±13.21	0.68±0.01	0.89±0.02	(5/5, 5/5)

Table 2: Competing risks prediction on the SEER and Rotterdam test sets. We report the mean and standard deviation, averaged over 5 experiments and the K events, except the censoring event. The mMAE scores on the Rotterdam dataset are divided by 100 for better readability. N is the number of samples, K is the number of events, and d is the number of covariates.

Dataset	Method	Harrell’s CI	IBS	mMAE	D-Cal
(SEER $N = 19,246$, $K = 2$, $d = 17$)	DeepSurv	0.76±0.0	0.15±0.0	29.23±0.6	0/5
	DeepHit	0.75±0.0	0.17±0.0	28.71±0.2	0/5
	MTLR	0.69±0.0	0.17±0.0	30.77±0.5	4/5
	DSM	0.75±0.0	0.15±0.0	41.95±3.3	2/5
	MENSA (Ours)	0.76±0.0	0.15±0.0	27.01±0.6	5/5
(MIMIC-IV $N = 26,236$, $K = 2$, $d = 100$)	DeepSurv	0.75±0.0	0.12±0.0	6.97±0.1	5/5
	DeepHit	0.74±0.0	0.14±0.0	6.43±0.1	0/5
	MTLR	0.72±0.0	0.13±0.0	7.65±0.5	0/5
	DSM	0.75±0.0	0.13±0.0	6.45±0.1	5/5
	MENSA (Ours)	0.75±0.0	0.13±0.0	5.70±0.1	0/5

Table 3: Single event prediction on SEER and MIMIC-IV test sets, averaged over 5 experiments and K events, excluding the censoring event. D-calibration counts the number of times the model was D-calibrated. The mMAE scores on the MIMIC-IV dataset are divided by 100 for better readability. N is the number of samples, K is the number of events, and d is the number of covariates.

cancer and death by heart failure. Furthermore, the proposed method is the only method that predicts D-calibrated survival curves across all five experiments for both the events. In the smaller Rotterdam dataset, we see a similar alignment between the proposed method and literature benchmarks in terms of discriminative performance. The proposed method has the second lowest mMAE score, and is aligned with rival algorithms in terms of global and local concordance-index, however, providing D-calibrated survival curves for both the relapse and death event.

Multi-event prediction

We now consider the task of predicting the time until functional decline in ALS patients. This is a multi-event survival problem, where the occurrence of one event does not exclude the others. Figure 3 shows prediction performance for each of the four events. In the first three cases, our method is better than state-of-the-art approaches at predicting when functional decline occurs in terms of the L1-Margin loss (mMAE). In the last case, our method is on par with Deep-

Surv. Most notably, our approach achieves an mMAE in days of 278.8 (95% CI 270.1-287.5) for the “Swallowing” event, compared to DeepSurv with 355.2 (95% CI 308.3-402.1) and the Hierarchical model with 602.324 (95% CI 594.2-610.3). We include the full results of this experiment in the Supplement.

6 Conclusion

We have presented MENSA, a novel method for survival analysis, that supports single-event, competing risks and multi-event scenarios. On both synthetic and real datasets, we showed that the proposed method led to improvements over well-accepted baselines in several performance metrics, especially in predictive accuracy. As a practical motivation for the multi-event case, we used our model to predict the time to functional decline in ALS patients, which in our case consisted of four distinct but related events. This application can facilitate the design of personalized treatment plans and provide insight into the relationship between covariates and outcome, better than simply predicting the time to death. Our method is also capable of predicting the censoring distribution, which enables medical practitioners to *e.g.*, predict if a patient is likely to drop out of a study.

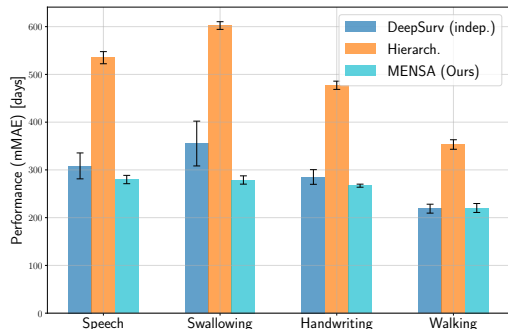


Figure 3: Model prediction for each event related to functional decline in ALS patients on the PRO-ACT test set. The error is reported in days. The error bars represent empirical 95% confidence intervals. Lower is better.

References

- Andersen, P. K.; and Keiding, N. 2002. Multi-state models for event history analysis. *Statistical Methods in Medical Research*, 11(2): 91–115.
- Armstrong, G. T.; Kawashima, T.; Leisenring, W.; Stratton, K.; Stovall, M.; Hudson, M. M.; Sklar, C. A.; Robison, L. L.; and Oeffinger, K. C. 2014. Aging and risk of severe, disabling, life-threatening, and fatal events in the childhood cancer survivor study. *Journal of Clinical Oncology*, 32(12): 1218.
- Atassi, N.; Berry, J.; Shui, A.; et al. 2014. The PRO-ACT database: design, initial analyses, and predictive features. *Neurology*, 83(19): 1719–1725.
- Cox, D. R. 1972. Regression models and life-tables. *Journal of the Royal Statistical Society: Series B (Methodological)*, 34(2): 187–202.
- Davidson-Pilon, C. 2019. lifelines: survival analysis in Python. *Journal of Open Source Software*, 4(40): 1317.
- Emura, T.; and Chen, Y.-H. 2018. *Analysis of Survival Data with Dependent Censoring: Copula-Based Approaches*. Springer.
- Foomani, A. H. G.; Cooper, M.; Greiner, R.; and Krishnan, R. G. 2023. Copula-based deep survival models for dependent censoring. In *Proceedings of the 39th Conference on Uncertainty in Artificial Intelligence*, volume 216, 669—680.
- Gareth, J.; Daniela, W.; Trevor, H.; and Robert, T. 2021. *An introduction to statistical learning: with applications in R*. Springer, 2 edition.
- Gloeckler Ries, L. A.; Reichman, M. E.; Lewis, D. R.; Hankey, B. F.; and Edwards, B. K. 2003. Cancer survival and incidence from the Surveillance, Epidemiology, and End Results (SEER) program. *Oncologist*, 8(6): 541–552.
- Graf, E.; Schmoor, C.; Sauerbrei, W.; and Schumacher, M. 1999. Assessment and comparison of prognostic classification schemes for survival data. *Statistics in medicine*, 18(17-18): 2529–2545.
- Gupta, M.; Gallamoza, B.; Cutrona, N.; Dhakal, P.; Poulain, R.; and Beheshti, R. 2022. An Extensive Data Processing Pipeline for MIMIC-IV. In *Proceedings of the 2nd Machine Learning for Health symposium*, volume 193, 311–325.
- Haider, H.; Hoehn, B.; Davis, S.; and Greiner, R. 2020. Effective Ways to Build and Evaluate Individual Survival Distributions. *Journal of Machine Learning Research*, 21(1): 1–63.
- Harrell Jr, F. E.; Lee, K. L.; and Mark, D. B. 1996. Multivariable prognostic models: issues in developing models, evaluating assumptions and adequacy, and measuring and reducing errors. *Statistics in medicine*, 15(4): 361–387.
- Hsieh, J.-J.; and Wang, J.-L. 2018. Quantile residual life regression based on semi-competing risks data. *Journal of Applied Statistics*, 45(10): 1770–1780.
- Ishwaran, H.; Kogalur, U. B.; Blackstone, E. H.; and Lauer, M. S. 2008. Random Survival Forests. *The Annals of Applied Statistics*, 2(3): 841–860.
- Jiang, F.; and Haneuse, S. 2017. A semi-parametric transformation frailty model for semi-competing risks survival data. *Scandinavian Journal of Statistics*, 44(1): 112–129.
- Johnson, A. E. W.; Bulgarelli, L.; Shen, L.; Gayles, A.; Shammout, A.; Horng, S.; Pollard, T. J.; Hao, S.; Moody, B.; Gow, B.; Lehman, L.-w. H.; Celi, L. A.; and Mark, R. G. 2023. MIMIC-IV, a freely accessible electronic health record dataset. *Scientific Data*, 10(1): 1–9.
- Kaplan, E. L.; and Meier, P. 1958. Nonparametric Estimation from Incomplete Observations. *Journal of the American Statistical Association*, 53(282): 457–481.
- Katzman, J.; Shaham, U.; Bates, J.; Cloninger, A.; Jiang, T.; and Kluger, Y. 2018. DeepSurv: personalized treatment recommender system using a Cox proportional hazards deep neural network. *BMC Medical Research Methodology*, 18(1): 1–12.
- Kim, S.; Kazmierski, M.; and Haibe-Kains, B. 2021. DeepCR MTLR: a Multi-Modal Approach for Cancer Survival Prediction with Competing Risks. In *Proceedings of AAAI Spring Symposium on Survival Prediction - Algorithms, Challenges, and Applications*, volume 146, 223–231.
- Kingma, D. P.; and Ba, J. 2017. Adam: A Method for Stochastic Optimization. arXiv:1412.6980.
- Kjældgaard, A. L.; Pilely, K.; Olsen, K. S.; Jessen, A. H.; Lauritsen, A. O.; Pedersen, S. W.; Svenstrup, K.; Karlsborg, M.; Thagesen, H.; Blaabjerg, M.; Theódórsdóttir, Á.; Elmo, E. G.; Møller, A. T.; Bonefeld, L.; Berg, M.; Garred, P.; and Møller, K. 2021. Prediction of survival in amyotrophic lateral sclerosis: a nationwide, Danish cohort study. *BMC Neurology*, 21(1): 164.
- Kuan, L.-H.; Parnianpour, P.; Kushol, R.; Kumar, N.; Anand, T.; Kalra, S.; and Greiner, R. 2023. Accurate personalized survival prediction for amyotrophic lateral sclerosis patients. *Scientific Reports*, 13(1): 20713.
- Larson, M. G. 1984. Covariate Analysis of Competing-Risks Data with Log-Linear Models. *Biometrics*, 40(2): 459–469.
- Lee, C.; and et al. 2019. Dynamic-Deephit: A deep learning approach for dynamic survival analysis with competing risks based on longitudinal data. *IEEE TBME*, 67(1): 122–133.
- Lee, C.; Zame, W.; Yoon, J.; and Van Der Schaar, M. 2018. Deephit: A deep learning approach to survival analysis with competing risks. In *Proceedings of the AAAI conference on artificial intelligence*, 1, 2314–2321.
- Li, Y.; Wang, J.; Ye, J.; and Reddy, C. K. 2016. A Multi-Task Learning Formulation for Survival Analysis. In *Proceedings of the 22nd ACM SIGKDD International Conference on Knowledge Discovery and Data Mining*, 1715–1724.
- Lillelund, C. M.; Magris, M.; and Pedersen, C. F. 2024. Efficient Training of Probabilistic Neural Networks for Survival Analysis. *IEEE Journal of Biomedical and Health Informatics*, 1–10.
- Ling, C. K.; Fang, F.; and Kolter, J. Z. 2020. Deep Archimedean Copulas. In *Advances in Neural Information Processing Systems*, volume 33, 1535–1545.

- Nagpal, C.; Li, X.; and Dubrawski, A. 2021. Deep survival machines: Fully parametric survival regression and representation learning for censored data with competing risks. *IEEE Journal of Biomedical and Health Informatics*, 25(8): 3163–3175.
- Paszke, A.; Gross, S.; Massa, F.; Lerer, A.; Bradbury, J.; Chanan, G.; Killeen, T.; Lin, Z.; Gimelshein, N.; Antiga, L.; Desmaison, A.; Kopf, A.; Yang, E.; DeVito, Z.; Raison, M.; Tejani, A.; Chilamkurthy, S.; Steiner, B.; Fang, L.; Bai, J.; and Chintala, S. 2019. PyTorch: An Imperative Style, High-Performance Deep Learning Library. In *Advances in Neural Information Processing Systems*, volume 32, 8026–8037.
- Qi, S.-a.; Kumar, N.; Farrokh, M.; Sun, W.; Kuan, L.; Ranganath, R.; Heno, R.; and Greiner, R. 2023. An Effective Meaningful Way to Evaluate Survival Models. In *Proceedings of the 40th International Conference on Machine Learning*, volume 202, 28244–28276.
- Qi, S.-a.; Kumar, N.; Xu, J.-Y.; Patel, J.; Damaraju, S.; Shen-Tu, G.; and Greiner, R. 2022. Personalized breast cancer onset prediction from lifestyle and health history information. *Plos one*, 17(12): e0279174.
- Qi, S.-a.; Sun, W.; and Greiner, R. 2023. SurvivalEVAL: A Comprehensive Open-Source Python Package for Evaluating Individual Survival Distributions. In *Proceedings of the 2023 AAAI Fall Symposia*, volume 2, 453–457.
- Royston, P.; and Altman, D. G. 2013. External validation of a Cox prognostic model: principles and methods. *BMC Medical Research Methodology*, 13: 33.
- Simon, R. M.; Korn, E. L.; McShane, L. M.; Radmacher, M. D.; Wright, G. W.; and Zhao, Y. 2003. *Design and analysis of DNA microarray investigations*, volume 209. Springer.
- Sklar, A. 1959. Fonctions de répartition à n dimensions et leurs marges. *Publications de l'Institut Statistique de l'Université de Paris*, 8: 229–231.
- Snoek, J.; Larochelle, H.; and Adams, R. P. 2012. Practical Bayesian Optimization of Machine Learning Algorithms. In *Advances in Neural Information Processing Systems*, volume 25, 2951–2959.
- Solomon, S. D.; Rizkala, A. R.; Gong, J.; Wang, W.; Anand, I. S.; Ge, J.; Lam, C. S.; Maggioni, A. P.; Martinez, F.; Packer, M.; et al. 2017. Angiotensin receptor neprilysin inhibition in heart failure with preserved ejection fraction: rationale and design of the PARAGON-HF trial. *JACC: Heart Failure*, 5(7): 471–482.
- Tjandra, D.; He, Y.; and Wiens, J. 2021. A Hierarchical Approach to Multi-Event Survival Analysis. *Proceedings of the AAAI Conference on Artificial Intelligence*, 35(1): 591–599.
- Tsiatis, A. A. 1975. A Nonidentifiability Aspect of the Problem of Competing Risks. *Proceedings of the National Academy of Sciences of the United States of America*, 72(1): 20–22.
- Wang, L.; Li, Y.; Zhou, J.; Zhu, D.; and Ye, J. 2017. Multi-task Survival Analysis. In *2017 IEEE International Conference on Data Mining (ICDM)*, 485–494.
- Wang, Z.; and Sun, J. 2022. SurvTRACE: transformers for survival analysis with competing events. In *Proceedings of the 13th ACM International Conference on Bioinformatics, Computational Biology and Health Informatics*.
- Yu, C.-N.; Greiner, R.; Lin, H.-C.; and Baracos, V. 2011. Learning Patient-Specific Cancer Survival Distributions as a Sequence of Dependent Regressors. In *Advances in Neural Information Processing Systems*, volume 24, 1845–1853.
- Zhang, W.; Ling, C. K.; and Zhang, X. 2024. Deep Copula-Based Survival Analysis for Dependent Censoring with Identifiability Guarantees. *Proceedings of the AAAI Conference on Artificial Intelligence*, 38(18): 20613–20621.

Supplementary Material

A - Notation

Table 4 provides a summary of the symbols and abbreviations used in this paper.

Symbol/Abbr.	Definition
$c_k^{(i)}$	Censoring time of observation i for event k
$e_k^{(i)}$	Event time of observation i for event k
$t_k^{(i)}$	Observed time of observation i for event k
$\delta_k^{(i)}$	Event indicator, $\delta_k^{(i)} = \mathbb{1}_{e_k^{(i)} > c_k^{(i)}}$
\mathcal{D}	Raw dataset
N	Number of observations in the dataset
d	Number of features/covariates in the dataset
$\mathbf{x}^{(i)}$	Covariates of observation i
$h_0(t)$	Baseline hazard function
$h(\cdot \mathbf{x}^{(i)})$	Hazard function given the covariates $\mathbf{x}^{(i)}$
K	Number of events
\mathcal{L}	Objective/loss function
B	Number of training epochs
$f(\boldsymbol{\theta}, \mathbf{x}^{(i)})$	Risk function given model parameters and covariates
$S_T \in \mathcal{S}$	Survival function, $S: \mathbb{R} \rightarrow [0, 1]$
\mathcal{S}	Space of survival functions
f_T	Probability density function, representing $\Pr(T = t)$
F_T	Cumulative density function, representing $\Pr(T < t)$
C_θ	A copula parameterized by θ
u_1, u_2	Inputs to a copula function
Abbreviations	
C-index	Concordance Index
IBS	Integrated Brier Score
D-Cal	Distribution Calibration
KM	Kaplan-Meier estimator
MAE	Mean Absolute Error
mMAE	Marginalized MAE

Table 4: Table of notation.

B - Evaluation metrics

Harrell’s CI: The concordance index (CI) measures the discriminative performance of a survival model by calculating the proportion of concordant pairs among all comparable pairs. A pair is considered comparable if we can determine who has the event first. It is defined as (Harrell Jr, Lee, and Mark 1996):

$$\text{C-index} = \frac{\sum_{i,j \in \mathcal{D}} \mathbb{1}_{t_i < t_j} \cdot \mathbb{1}_{\eta_i > \eta_j} \cdot \delta_i}{\sum_{i,j \in \mathcal{D}} \mathbb{1}_{t_i < t_j} \cdot \delta_i}, \quad (13)$$

where η_i and η_j represent risk scores for individuals i and j , respectively.

Global CI: The global CI is calculated as the average of the C-index values across all specific events, providing an overall measure of a model’s discriminative performance for all competing and multiple events. This approach follows previous work (Lee et al. 2018; Katzman et al. 2018), ensuring a comprehensive evaluation of the model’s global discrimination ability. It is defined as:

$$\text{Global CI} = \frac{\sum_{k \in K} \sum_{i,j \in \mathcal{D}_k} \mathbb{1}_{t_i < t_j} \cdot \mathbb{1}_{\eta_i > \eta_j} \cdot \delta_i}{\sum_{k \in K} \sum_{i,j \in \mathcal{D}_k} \mathbb{1}_{t_i < t_j} \cdot \delta_i}, \quad (14)$$

where K represents the set of all distinct events, and the index k corresponds to the k -th specific event.

Local CI: The local CI is computed by averaging C-index scores across multiple events for each instance, as introduced by Tjandra, He, and Wiens (2021). The Local CI evaluates the model’s ability to discriminate between multiple events within a single instance. It is defined as:

$$\text{Local CI} = \frac{\sum_{i \in N} \sum_{k_1, k_2 \in \mathcal{K}_i} \mathbb{1}_{t_{k_1} < t_{k_2}} \cdot \mathbb{1}_{\eta_{k_1} > \eta_{k_2}} \cdot \delta_{k_1}}{\sum_{i \in N} \sum_{k_1, k_2 \in \mathcal{K}_i} \mathbb{1}_{t_{k_1} < t_{k_2}} \cdot \delta_{k_1}}, \quad (15)$$

where \mathcal{K}_i represents the set of all K different events for instance i , and η_{k_1} and η_{k_2} denote the risk scores associated with the two events, respectively.

BS/IBS: The Brier Score (BS) is defined as the mean squared difference between the predicted survival curve and the Heaviside step function of the observed event. The Integrated Brier Score (Graf et al. 1999) (IBS) aggregates the Brier Scores across multiple time points to provide a single measure of model performance. We use inverse probability weighting (IPCW) to handle censored events. The BS is defined as:

$$\text{BS}(t^*) = \frac{1}{N} \sum_{i \in \mathcal{D}} \left[\frac{S(t^* | \mathbf{x}_i)^2 \cdot \mathbb{1}_{t_i \leq t^*, \delta_i = 1}}{G(t_i)} + \frac{(1 - S(t^* | \mathbf{x}_i))^2 \cdot \mathbb{1}_{t_i > t^*}}{G(t^*)} \right], \quad (16)$$

which is the mean square error between observe survival status and survival probability at time t^* and where $G(t^*)$ is the non-censoring probability at time t^* . The IBS is defined as:

$$\text{IBS} = \frac{1}{N} \sum_{i \in \mathcal{D}} \frac{1}{t_{\max}} \cdot \int_0^{t_{\max}} \text{BS}(t) dt, \quad (17)$$

where t_{\max} is the maximum observed time.

MAE: The mean absolute error (MAE) is the absolute difference between the predicted and actual survival times. Given an individual survival distribution, $S(t | \mathbf{x}_i) = \Pr(T > t | \mathbf{x}_i)$, we calculate the predicted survival time \hat{t}_i as the median survival time (Qi, Sun, and Greiner 2023):

$$\hat{t}_i = \text{median}(S(t | \mathbf{x}_i)) = S^{-1}(\tau = 0.5 | \mathbf{x}_i), \quad (18)$$

$$\text{MAE}(\hat{t}_i, t_i, \delta_i = 1) = |t_i - \hat{t}_i|. \quad (19)$$

For censored individuals, we calculate the marginal MAE (mMAE) as proposed by Haider et al. (2020):

$$\text{mMAE} = \frac{1}{\sum_{i=1}^N \omega_i} \sum_{i=1}^N \omega_i \left| [(1 - \delta_i) \cdot e_m(t_i) + \delta_i \cdot t_i] - \hat{t}_i \right|,$$

$$\text{where } e_m(t_i) = \begin{cases} t_i + \frac{\int_{t_i}^{\infty} S_{\text{KM}}(t) dt}{S_{\text{KM}}(t)} & \text{if } \delta_i = 0 \\ t_i & \text{if } \delta_i = 1 \end{cases},$$

$$\text{and } \omega_i = \begin{cases} 1 - S_{\text{KM}}(t_i) & \text{if } \delta_i = 0 \\ 1 & \text{if } \delta_i = 1 \end{cases}. \quad (20)$$

D-calibration: Distribution calibration (Haider et al. 2020) measures the calibration performance of $S(t)$, expressing to what extent the predicted probabilities can be trusted. We assess this using a Pearson’s χ^2 goodness-of-fit test. For any probability interval $[a, b] \in [0, 1]$, we define $D_m(a, b)$ as the group of individuals in the dataset D whose predicted probability of event is in the interval $[a, b]$ (Qi et al. 2023). A model is D-calibrated if the amount of individuals $|D_m(a, b)|/|D|$ is statistically similar to the amount $b - a$.

Survival- ℓ_1 : The Survival- ℓ_1 metric is the ℓ_1 distance between the ground-truth survival curve, $S_{T|X}$, and the estimated survival curve, $\hat{S}_{T|X}$, over the event horizon (Foomani et al. 2023). We normalize the area between the survival curves by $T_{\max}^{(i)} = S_{T|X}^{-1}(Q|| \cdot ||)$ to ensure that the duration spanned by a patient’s survival curve does not influence that patient’s contribution to the metric relative to other patients. The Survival- ℓ_1 is thus denoted:

$$C_{\text{Survival-}\ell_1}(S, \hat{S}) = \frac{1}{N} \sum_{i=1}^N \frac{1}{T_{\max}^{(i)}} \int_0^\infty \left| S_{T|X}(t | X^{(i)}) - \hat{S}_{T|X}(t | X^{(i)}) \right| dt. \quad (21)$$

C - Copulas

Copulas are functions of d -dimensional multivariate distributions with uniform margins. Let $C_\theta : [0, 1]^2 \rightarrow [0, 1]$ be a bivariate copula indexed by a parameter θ . By definition, any bivariate copula satisfies the following conditions (Emura and Chen 2018, Ch. 3):

- **(C1)** $C_\theta(u, 0) = C_\theta(0, v) = 0$, $C_\theta(u, 1) = u$, and $C_\theta(1, v) = v$ for $0 \leq u \leq 1$ and $0 \leq v \leq 1$.
- **(C2)** $C_\theta(u_2, v_2) - C_\theta(u_2, v_1) - C_\theta(u_1, v_2) + C_\theta(u_1, v_1) \geq 0$ for $0 \leq u_1 \leq u_2 \leq 1$ and $0 \leq v_1 \leq v_2 \leq 1$.

Condition **(C1)** requires the uniformity of the two marginal distributions. Condition **(C2)** requires that C_θ produces a probability mass on the rectangular region $[u_1, u_2] \times [v_1, v_2]$. Among others, the following copulas used in this work meet Conditions (C1) and (C2) (Emura and Chen 2018, Ch. 3):

- **The Independence copula:** $C(u, v) = uv$.
- **The Clayton copula:**

$$C_\theta(u, v) = (u^{-\theta} + v^{-\theta} - 1)^{-1/\theta}, \quad \theta \geq 0.$$

- **The Frank copula:**

$$C_\theta(u, v) = -\frac{1}{\theta} \log \left[1 + \frac{(e^{-\theta u} - 1)(e^{-\theta v} - 1)}{e^{-\theta} - 1} \right], \quad \theta \neq 0.$$

Abe Sklar introduced the most fundamental theorem about copulas, Sklar’s theorem, which states that any d -dimensional continuous joint distribution can be uniquely expressed with d -uniform marginals and a copula C :

Theorem 1 (Sklar 1959) Let F be a distribution function with margins F_1, \dots, F_d , then there exists a d -dimensional copula C such that for any $(x_1, \dots, x_d) \in \mathbb{R}^d$ we have

$$F(x_1, \dots, x_d) = C(F_1(x_1), \dots, F_d(x_d)). \quad (22)$$

Furthermore, if the marginals F_1, \dots, F_d are continuous, C is unique.

D - Data Preprocessing Details

Synthetic: This paper utilizes two synthetic datasets with 3 competing risk events – one linear and the other non-linear, both based on the semi-parametric Weibull distribution as discussed in Foomani et al. (2023). The datasets are characterized by the conditional hazard function and conditional survival probability of an event $T | X$ as follows:

$$h_{T|X}(t | X) = \left(\frac{v}{\rho} \right) \left(\frac{t}{\rho} \right)^{v-1} \exp(g_\Psi(X)),$$

$$S_{T|X}(t | X) = \exp \left(- \left(\frac{t}{\rho} \right)^v \exp(g_\Psi(X)) \right), \quad (23)$$

where v and ρ represent the shape and scale parameters of the Weibull distribution, respectively. The function $g_\Psi(X)$ represents the risk function, which is a linear function for the linear dataset and a two-layer neural network with sine activation for the non-linear dataset.

The data generation process begins by initializing a copula with a predefined parameter θ . We then sample N sets of CDF observations from the copula, each containing three CDF probabilities (corresponds to each competing event). From these probabilities, we then calculate the corresponding times using the inverse function of (23). This data generation process has been described in Algorithm 2 in Foomani et al. (2023).

MIMIC-IV: We utilized the MIMIC-IV v2.2 dataset (Johnson et al. 2023), which includes data on 299,712 patients and 431,231 admissions. Preprocessing was conducted using the MIMIC-IV Pipeline method (Gupta et al. 2022), through which we extracted 1,672 static features from the dataset. To focus our analysis, we filtered the dataset to include only 26,236 patients aged between 60 and 65 years. For feature refinement, we applied the Unicox feature selection method (Qi et al. 2022; Simon et al. 2003). In the training set, we assessed the statistical significance of each feature by calculating the p-values using lifelines’ (Davidson-Pilon 2019) CoxPHFitter summary. The top 100 features with the smallest p-values, indicating the highest relevance, were selected. The event of interest in our study is mortality following hospital admission. The final set of features is included in the source code.

SEER: Surveillance, Epidemiology, and End Results (SEER) Program dataset (Gloeckler Ries et al. 2003) is a comprehensive collection of clinical data in the United States. This dataset, which encompasses about 49% of the U.S. population, includes vital information on patient diagnoses, time until an event happens, and other relevant details sourced from various registries. We use the raw feature “COD to site recode” to extract the event indicator. In particular, we focus on two types of events: breast cancer and

Method	Event	Harrell’s CI	IBS	mMAE	Global CI	Local CI	D-Cal
DeepSurv (indep.)	Speech	0.63±0.02	0.17±0.01	308.40±19.55	0.60±0.01	0.76±0.01	(0/5)
	Swallowing	0.64±0.01	0.17±0.01	355.22±33.80	0.60±0.01	0.76±0.01	(4/5)
	Handwriting	0.59±0.01	0.18±0.00	285.20±11.06	0.60±0.01	0.76±0.01	(5/5)
	Walking	0.56±0.01	0.15±0.01	218.84±6.73	0.60±0.01	0.76±0.01	(5/5)
Hierarch.	Speech	0.63±0.01	0.49±0.01	535.00±9.14	0.59±0.01	0.68±0.02	(0/5)
	Swallowing	0.65±0.01	0.55±0.00	602.32±5.80	0.59±0.01	0.68±0.02	(0/5)
	Handwriting	0.58±0.01	0.45±0.01	477.23±6.23	0.59±0.01	0.68±0.02	(0/5)
	Walking	0.53±0.01	0.34±0.01	353.20±7.19	0.59±0.01	0.68±0.02	(0/5)
MENSA	Speech	0.62±0.02	0.18±0.00	279.84±6.28	0.58±0.01	0.75±0.01	(0/5)
	Swallowing	0.64±0.01	0.18±0.00	278.88±6.26	0.58±0.01	0.75±0.01	(5/5)
	Handwriting	0.56±0.01	0.18±0.01	266.97±2.31	0.58±0.01	0.75±0.01	(5/5)
	Walking	0.52±0.01	0.16±0.01	220.26±6.74	0.58±0.01	0.75±0.01	(1/5)

Table 5: Multi-event prediction results on the PRO-ACT test set. All experiments were conducted five times with different randomization seeds. D-Cal reports the number of times the model was D-calibrated for the respective event and seed. The proposed method is generally better at predicting the time to event, indicated by lower mMAE score, than the independent DeepSurv model and the Hierarchical model, while rivaling their performances in the concordance-indices.

heart disease. Then, we apply some special value processing for some features, based on the guideline provided by Wang and Sun (2022). For categorical features, missing values are imputed using the mode, followed by one-hot encoding. The data is then standardized to ensure consistency in our analyses.

Rotterdam: The Rotterdam dataset (Royston and Altman 2013) consists of records from 2,982 primary breast cancer patients included in the Rotterdam tumor bank, with 1,546 of these patients having node-positive disease. The dataset contains 10 covariates, encompassing demographic information, tumor characteristics, and treatment details. Survival time is defined as the duration from primary surgery to the occurrence of either disease recurrence or death from any cause, representing two competing risks.

During preprocessing, categorical size groups (≤ 20 , $20 - 50$, > 50) were converted to their approximate median values (10, 35, 75, respectively). Additionally, the remaining features were normalized to ensure consistency across the dataset.

PRO-ACT: The PRO-ACT dataset (Atassi et al. 2014) can be downloaded from their website (<https://ncr1.partners.org/ProACT>). An account is required for access. Data was downloaded on the 13th April 2024. The dataset contains over 8,500 clinical ALS patient records, including demographic, lab, family history and medical data. Data were extracted from the following files:

- PROACT_ALSFERS.csv
- PROACT_ALSHISTORY.csv
- PROACT_FVC.csv
- PROACT_HANDGRIPSTRENGTH.csv
- PROACT_MUSCLESTRENGTH.csv
- PROACT_ELESCORIAL.csv

To annotate events, we consider the first visitation a patient has as the baseline visitation and calculate the number of days from the baseline to the follow-up visitation. Considering the four events of interest, “Speech”, “Swallow-

ing”, “Handwriting”, and “Walking”, if the patient’s ALSFRS score has dropped to a 2 or below at the point of follow-up in any of the four categories, this is considered a positive event for that category. We encode the categorical feature “Site_of_Onset” as an integer array. Forced Vital Capacity (FVC) scores are recorded as minimum, maximum and mean values. In some patients, muscle strength tests are performed to measure the isometric strength of different muscle groups in the arms, legs, and hips using a hand-held dynamometer. Handgrip strength is measured in kilograms, while other muscle strength tests use Newtonmeters. The provided strength tests cover the following muscle groups: “Hand”, “Elbow”, “Knee”, “Shoulder”, “First dorsal interosseous of the hand”, “Wrist”, “Ankle” and “Hip flexor”. Lastly, we include the El Escorial Criteria (EEC) as a covariate, which establishes the likelihood of disease based on clinical findings. The code for preprocessing the data is available in the source code repository.

E - Results on the PRO-ACT dataset

Table 5 shows detailed results for predicting the time until functional decline in ALS patients for four separate events (“Speech”, “Swallowing”, “Handwriting” and “Walking”). We show the prediction results for each event separately.

F - Model Hyperparameters

Table 6 reports the selected hyperparameters for the MENSA model. We use the same hyperparameters for single-event, competing risks and multi-event settings. We use Bayesian optimization (Snoek, Larochelle, and Adams 2012) to tune hyperparameters over ten iterations on the validation set, adopting the hyperparameters leading to the lowest likelihood loss.

We use sensible default hyperparameters for the literature benchmarks by consulting the original work. Hyperparameters for the literature benchmarks are outlined below.

Hyperparameter	Synthetic	SEER	Rotterdam	MIMIC-IV	PRO-ACT
Batch size	32	128	32	32	128
# Nodes per layer	[32]	[128]	[32]	[32]	[16]
Learning rate	$1e-4$	$5e-4$	$1e-3$	$1e-3$	$1e-3$
Number of dists.	3	3	1	1	1

Table 6: MENSA hyperparameters.

Table 7: CoxPH hyperparameters.

Parameter	Value
alpha	0
ties	breslow
n_iter	100
tol	$1e-9$

Table 8: RSF hyperparameters.

Parameter	Value
n_estimators	100
max_depth	3
min_samples_split	60
min_samples_leaf	30
max_features	None
random_state	0

Table 9: DeepSurv hyperparameters.

Parameter	Value
hidden_size	32
verbose	False
lr	0.005
c1	0.01
num_epochs	1000
dropout	0.25
batch_size	32
early_stop	True
patience	10

Table 10: DeepHit hyperparameters.

Parameter	Value
num_nodes_shared	[32]
num_nodes_indiv	[32]
batch_norm	True
verbose	False
dropout	0.25
alpha	0.2
sigma	0.1
batch_size	32
lr	0.001
weight_decay	0.01
eta_multiplier	0.8
epochs	1000
early_stop	True
patience	10

Table 11: DSM hyperparameters.

Parameter	Value
network_layers	[32]
learning_rate	0.001
n_iter	10000
k	3
batch_size	32

Table 12: DCSurvival hyperparameters.

Parameter	Value
depth	2
num_epochs	1000
widths	[100, 100]
lc_w_range	[0, 1.0]
shift_w_range	[0.0, 2.0]
learning_rate	$1e-4$

G - Reproducibility

All experiments were implemented and conducted in Python 3.9 with PyTorch 1.13.1, NumPy 1.24.3 and Pandas 1.5.3 on a single workstation with an Intel Core i9-10980XE 3.00GHz CPU, 64GB of memory, and an NVIDIA GeForce RTX 3090 GPU. CUDA 11.7 was used to perform model training on the GPU. The source code repository contains the source code and information on how to reproduce the results. All datasets used in this study are publicly available. The MIMIC-IV, SEER and PRO-ACT datasets can be obtained from their respective websites by following the citation provided. The Rotterdam dataset is included in the source code folder.

Table 13: Hierarchical hyperparameters.

Parameter	Value
theta_layer_size	[100]
layer_size_fine_bins	[(50, 5), (50, 5)]
lr	0.001
reg_constant	0.05
n_batches	10
batch_size	32
backward_c_optim	False
hierarchical_loss	True
alpha	0.0001
sigma	10
use_theta	True
use_deephit	False
n_extra_bins	1
verbose	True

Table 14: MTLR hyperparameters.

Parameter	Value
hidden_size	32
verbose	False
lr	0.001
c1	0.01
num_epochs	1000
dropout	0.5
batch_size	32
early_stop	True
patience	10

Table 15: MTLRCR hyperparameters.

Parameter	Value
hidden_size	32
verbose	False
lr	1e-3
c1	0.01
num_epochs	1000
dropout	0.25
batch_size	32
early_stop	True
patience	10